Uluslararası İleri Doğa Bilimleri ve Mühendislik Araştırmaları Dergisi
Sayı 7, S. 396-402, 10, 2023

Araştırma Makalesi

IJANSER
https://alls-academy.com/index.php/ijanser
ISSN: 2980-0811

International Journal of Advanced Natural Sciences and Engineering Researches
Volume 7, pp. 396-402, 10, 2023

Research Article

Adsorption of cationic dyes with electrospun adsorbent fibers

A.I. Abdul Jalil[1], M. Shahadat[2] and S. Ismail[1]

[1] *School of Chemical Engineering, Engineering Campus, Universiti Sains Malaysia, 14300 Nibong Tebal, Pulau Pinang, Malaysia.*
[2]*School of Chemical Sciences, 11800, Universiti Sains Malaysia, Pulau Pinang, Malaysia*

[*]*chsuzy@usm.my*

(Received: 19 November 2023, Accepted: 26 November 2023)

(4th International Conference on Engineering and Applied Natural Sciences ICEANS 2023, November 20-21, 2023)

ATIF/REFERENCE: Jalil, A. I. A., Shahadat, M. & Ismail, S. (2023). Adsorption of cationic dyes with electrospun adsorbent fibers. *International Journal of Advanced Natural Sciences and Engineering Researches*, 7(10), 396-402.

Abstract **–** The use of electrospun fiber using polyacrylonitrile (PAN) as an adsorbent is a promising premise in the treatment of dyed wastewater, such as brilliant green dye, from the environment. Electrospinning is the technology where polymer solutions can be formed into micro to nano-sized fibers that contain massive potential in wastewater treatment technology. In the present study, PAN/Bentonite (PAN/Ben) was prepared by suspending bentonite powder in PAN solution before the electrospinning process. The composite electrospun adsorbent fiber is then used for treating cationic dye wastewater. The composition and morphology study of the adsorbent fiber found that the diameter of the fibers formed at 3.42 µm with elements of bentonite embedded in it. The adsorption ability of the adsorbent fibers reached 96% removal of 100 ppm dye concentration, with 64.84 mg/g adsorption capacity. The batch adsorption analysis demonstrated that the adsorption process followed the Langmuir isotherm best, showing that the adsorption process consists of monolayer adsorption on the surface of the adsorbent fiber. The experimental data fits better in the pseudo-second order kinetic model, proving the adsorption to be chemisorption. The pH and temperature study found that the adsorbent performs better as the pH levels increase from neutral to basic conditions, meanwhile the fiber adsorption ability improves as the temperature of the solution increase. The present work can provide new ways to utilize the electrospinning technology for adsorption fibers.

Keywords – Polyacrylonitrile; Bentonite; Electrospinning; Adsorption; Cationic Dye

I. INTRODUCTION

Batik is one of the fastest growing industry in Malaysia which contributes to the economic growth of the country. The textile industry increased the GDP of Malaysia up to 93.6% in 2021 alone [1]. However, with increased production of textile, comes the increased production of scheduled waste, where Malaysia produced 7249.40 MT/year if schedule waste in 2020 [2]. The United Nations World Water Development report stated that 80% of the wastewater from these sectors is released to the environment with appropriate treatment [3]. The release of the dye water affects both the groundwater and soil. With repeated uncontrolled dye wastewater release, the contamination of the soil and water source reduces the nutrients of the soil, affects the health of aquatic creatures, and hinders the photosynthesis of underwater plants [4].

Thus, wastewater treatment is a serious issue that has been studied by many scientists such as [5]–[9]. One of the typically used approach to treat these wastewaters is by the use of the adsorption technology [10]–[13]. Various adsorbents, such as activated carbon [14], [15], natural clay [16]–[18] and polymer membranes or fibers [19], [20] have been employed in water remediation studies. Polyacrylonitrile (PAN), a synthetic polymer, have been used in water purification due to its high mechanical strength, high degree of molecular orientation and flexibility [21], [22]. Additionally, PAN is also compatible in electrospinning as well. However, PAN lack in necessary functional group limits its adsorption ability, thus reducing its efficiency. To overcome this weakness, physical blending of adsorbents into the polymer is one of the ways. Bentonite, known for its strong adsorption capacity, can be introduced into the polymer through this method, providing additional active adsorption sites. The negative charge is induced by isomorphous substitution of Al3+ for Si4+ in the tetrahedral layer and Mg2+ for Al3+ in the octahedral layer. Moreover, the existence of exchangeable cations such as Na+ and Ca2+ in the lattice structure enables the bentonite in adsorbing cationic contaminants by ionic exchange [23].

Following this reasoning, PAN polymer can be electrospun with bentonite as its filler, increasing its ability to treat dye wastewater. Electrospinning is a technology with increasing interest due to its ability to produce highly efficient adsorbent, having fibrous structure along with high specific surface area, and ease of use [24]. Using electrospinning, a nanofiber made from a mixture of PAN polymer and bentonite can be created. Few studies have been reported using bentonite as the filler for PAN nanofiber for the treatment of cationic dyes. Therefore, in the present study, electrospun PAN/Ben nanofibers were prepared by mixing PAN solution with bentonite clay until homogeneity before undergoing the electrospinning process. The physicochemical properties of the resultant PAN/Ben nanofiber were characterized by scanning electron microscope (SEM), and Fourier-transform infrared spectroscopy (FTIR). To evaluate the adsorption behaviour of PAN/Ben nanofiber for the removal of BG dye, the effects of adsorbent dosage, adsorbate concentration, pH, adsorption kinetics, and adsorption isotherm were studied.

II. Materials and Method

a) Reagents and chemicals

Brilliant green (BG) dye (purity of 90%, colour index 42040, molecular weight of 482.63 g/mol λ_{max} = 625 nm, CAS:2734-67-6, molecular formula = $C_{27}H_{34}N_2O_4S$) was supplied from Chemolab Supplies Sdn. Bhd. BG dye acts as the cationic adsorbate, in an aqueous solution. Polyacrylonitrile powder (MW = 150 000 g/mol), and bentonite clay powder was purchased from Biotek Abadi Sdn. Bhd. Dimethyl sulfoxide (DMSO) which acts as the solvent for the polymer was acquired from BT Science Sdn. Bhd. Distilled water was used for the preparation of an aqueous dye solution. The pH of solutions was adjusted by NaOH and HCl solutions (0.1 M) purchased from Merck, Malaysia. The stock solution of BG dye was prepared by weighting 1 g with an analytical balance (A&D Company, model HR-250A) and then dissolved completely in 1 L of distilled water. Dilution is then used to obtain various adsorbate concentrations for subsequent adsorption tests. The adsorbate concentration was measured using UV-VIS spectroscopy (model Shimadzu UV-1800) where the calibration curve of the BG dye was obtained from 50 – 250 mg/L at 625 nm.

b) Preparation of PAN/Ben nanofibers, and physicochemical characterization.

PAN/Ben nanofiber was synthesized from PAN solution and commercial bentonite clay powder. Initially, 9% w/v PAN solution was prepared with 40 mL of DMSO solution at 55 ℃ and ℃ then magnetically stirred for 8 h. The bentonite powder was then added to the PAN solution and stirred until homogeneity. The homogenous solution was then electrospun using the electrospinning equipment (Progene Link Sdn. Bhd.). The electrospinning parameter was set to 11 kV voltage, a flow rate of 1 mL/h, tip-to-collector distance of 12 cm. The resultant nanofiber was dried at 55 ℃ for 1 h. The material was used as the adsorbent in BG dye adsorption tests.

The surface morphology of PAN nanofiber before and after the addition of bentonite was characterized by Scanning Electron Microscope SEM/EDX (FEI model Quanta 450 FEG). The changes in the functional groups of the PAN

nanofiber were determined in the region of 4000-400 cm^{-1} with a spectral resolution of 4 cm^{-1} using FTIR spectroscopy (Shimadzu model IR Prestige-21). The surface area and pore volume of the PAN/Ben nanofiber were estimated via nitrogen adsorption at 22 ℃ using a BET surface analyzer (Micrometrics model ASAP 2000, Nocross, GA).

c) Batch adsorption experiments, kinetics, and isotherms

Batch adsorption experiments were carried out to evaluate the PAN/Ben nanofiber performance for BG dye removal. The adsorbent performance was studied by analyzing various operating factors such as initial adsorbent concentration (1 to 7 wt%) initial adsorbate concentration (50 to 250 mg/L), adsorption temperature (25 to 100 ℃) and solution pH (2 to 10). All experiments were performed with 50 mL of BG dye solution until the nanofiber adsorbent reached equilibrium (i.e., 3 h of contact time). The adsorption capacities in all the experiments were estimated via an adsorbate material balance using the equation:

$$q = \frac{(C_O - C_f)V}{W} \quad (1)$$

where C_O and C_f are initial and final concentrations (mg/L) of the BG dye adsorption experiment respectively, V is the volume of adsorbate solution (L), and W is the mass of the nanofiber (g). The adsorption capacities at time t (h) and equilibrium state are denoted as q_t and q_e (mg/g) respectively.

BG dye adsorption isotherms and kinetics with PAN/Ben nanofiber were also quantified and stated in Table 1. Kinetics were determined with initial BG dye concentrations from 50 – 250 mg/L at actual pH and 30 ℃ under stirring of 500 rpm. Other than that, the PAN/Ben adsorption isotherm was conducted at 25 – 100 ℃ and actual pH using a contact time of 3 h. Both kinetic and isotherm experiments were done with 0.3 g of adsorbent dosage.

Therefore, the experimental data for the PAN/Ben adsorption was correlated with the Langmuir and Freundlich isotherm model and the pseudo-first-order and pseudo-second-order kinetic models were used to fit the experimental data. The summary of each model is given in Table 1 and explanations of each model can be found in the references. Model parameters of K_L and K_T are the adsorption constants of each isotherm equation given in L/mg, while K_F is the adsorption constant for Freundlich isotherm given in unit $(mg/g)\cdot(L/mg)^{1/n}$. q_{max} is the maximum adsorption capacity (mg/g), and 1/n is the adsorption intensity. The model parameters for each isotherm equation are as follows:

Table 1. Isotherm and kinetics used for the analysis of BG dye adsorption on PAN/Ben fiber

Isotherm models		Reference	Equation
Langmuir	$q_e = \frac{q_{max}K_L C_e}{1 + K_L C_e}$	[25]	(2)
Freundlich	$q_e = K_F C_e^{1/n}$	[25]	(3)
Kinetic models		Reference	Equation
Pseudo-first-order	$q_t = q_e(1 - e^{-k_1 t})$	[26]	(4)
Pseudo-second-order	$q_t = \frac{q_e^2 k_2 t}{1 + q_e K_2 t}$	[26]	(5)

III. RESULTS

3.1 Physicochemical characterization of PAN/Ben nanofiber

The surface morphology of PAN nanofiber and PAN/Ben nanofiber is shown in Figure 1. The normal PAN nanofiber surface shows a thin fibrous fiber (368.88 nm) with a criss-cross pattern. Meanwhile, the bentonite-infused PAN shows a thicker fiber (3.42 μm). The irregularity became more uniform as bentonite was integrated into the fiber and the thickness of the fiber increased. The SEM-EDX of each fiber is reported in Table 2, which indicates the major element composition is composed of carbon. The aluminium and silica were identified in the adsorbent point to the presence of bentonite. The specific surface area and pore volume of PAN/Ben nanofiber were 43.52 m^2/g

0.006 cm^3/g, respectively. Figure 2 reports the FTIR spectra for the PAN/Ben nanofiber to identify the functional groups of the PAN polymer and bentonite. The band of OH stretching at 3442 cm^{-1} of structural hydroxyl groups and water present in the mineral [27]. The H-O-H bending vibration is shown at 1666.65 cm^{-1} and CH_2 scissoring can be found at 1425.40 cm^{-1} [28]. The peaks at 1031.92, 947.06, 696.23 and 663.51 cm^{-1} show the vibrational modes of Si-O stretching and show the characteristic of layered silicate montmorillonite mineral.

Table 2 : Result of the elemental analysis (SEM-EDX) of PAN and PAN/Ben nanofiber

Elements	Weight %	
	PAN	PAN/Ben
Carbon, C	100	76.36
Oxygen, O	N/A	15.23
Aluminium, Al	N/A	1.36
Silica, Si	N/A	6.30
Sulphur, S	N/A	0.75

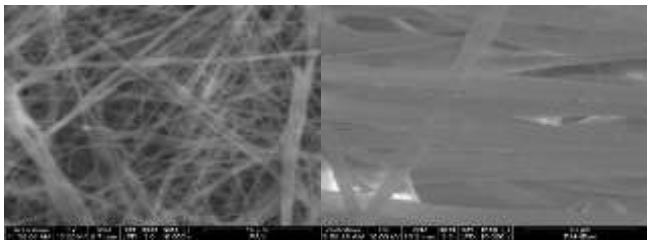

Figure 1 : Surface morphology of (a) PAN nanofiber and (b) PAN/Ben nanofiber

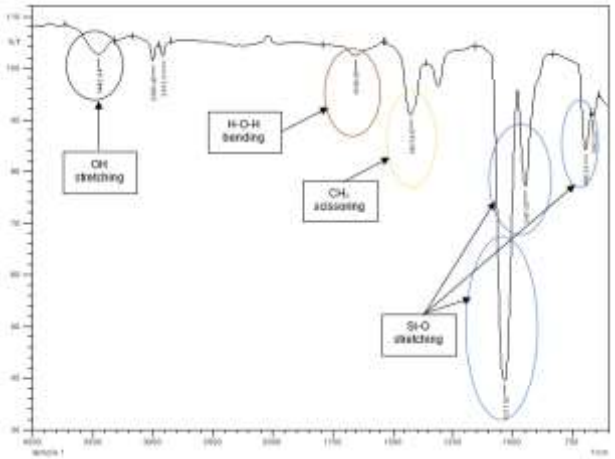

Figure 2. FTIR result of PAN/Ben nanofiber

3.2 Impact of adsorption operating conditions on BG dye removal with PAN/Ben nanofiber: kinetic and isotherms

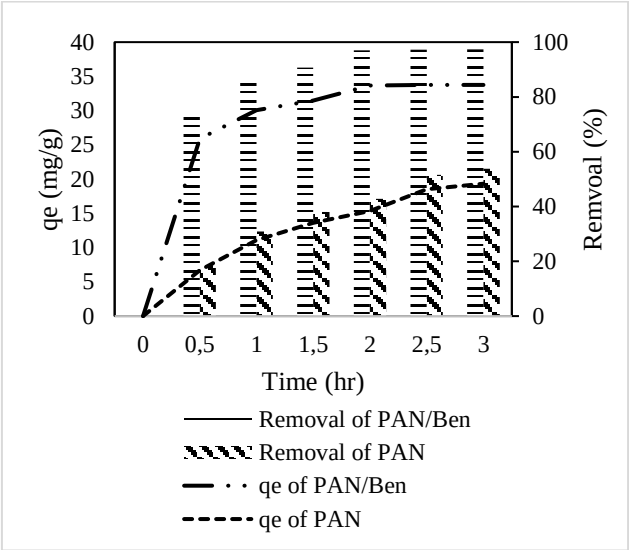

Figure 3. Impact of addition of bentonite to PAN on the BG dye removal and adsorption capacity at 303 K, 50 ppm adsorbate concentration, actual pH and 500 rpm of stirring

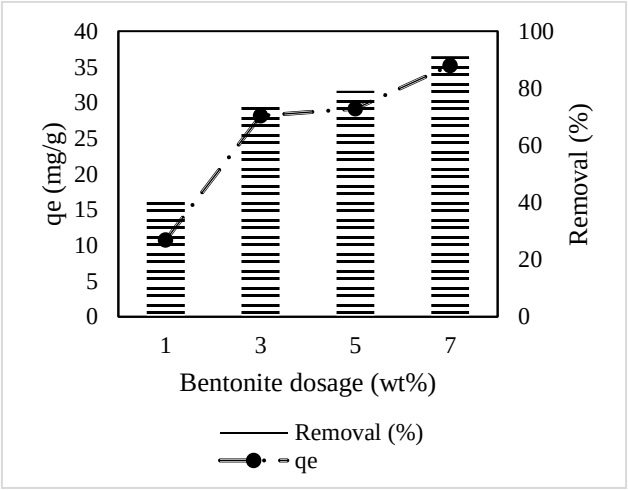

Figure 4. Impact of increasing bentonite dosage on BG dye removal and adsorption capacity at 303 K, 50 ppm adsorbate concentration, actual pH and 500 rpm of stirring

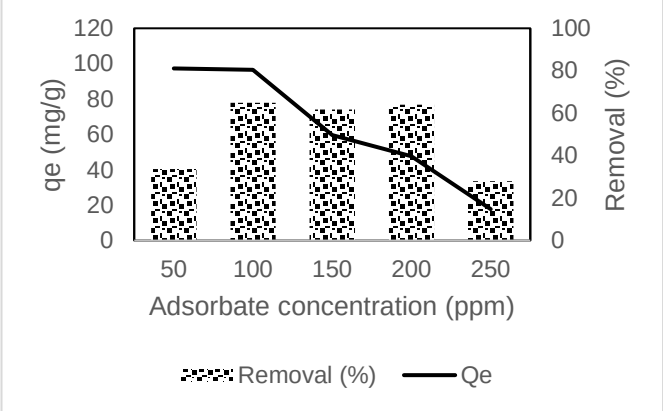

Figure 5. Impact of adsorbate concentration on the BG dye removal and adsorption capacity of PAN/Ben nanofiber at 303 K, actual pH and 500 rpm of stirring

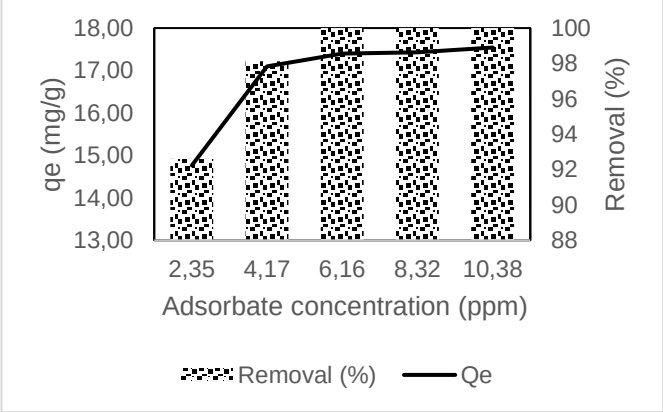

Figure 2. Impact of pH on the BG dye removal and adsorption capacity of PAN/Ben nanofiber at 303 K, 50 ppm adsorbate concentration and 500 rpm of stirring.

Table 3. Result of isotherm models for the BG dye adsorption on the PAN/Ben nanofiber at actual pH

Parameter	Temperature (K)			
	303	323	348	373
Langmuir isotherm				
q_{max} (mg/g)	20.54	26.53	30.21	59.17
K_L (L/mg)	3.36	0.21	0.81	0.35
R^2	0.78	0.97	0.99	0.93
Freundlich isotherm				
1/n	0.03	0.20	0.09	0.31
K_F ((mg/g).(L/mg)$^{1/n}$)	18.86	11.36	20.86	19.89
R^2	0.04	0.75	0.46	0.97

IV. DISCUSSION

The effect of PAN nanofiber and PAN/Ben nanofibers were studied to identify the adsorption capacity and removal performance (%) of cationic BG dye using fixed adsorbate concentration (50 mg/L) at 303 K and actual pH under 400 rpm of stirring. Figure 3 shows the effect of the addition of bentonite to the PAN solution. It was found that the removal performance had increased from 53 to 97% removal. In addition, the BG dye adsorption capacity increased from 19.32 to 33.72 mg/g with the addition of bentonite. Meanwhile, Figure 4 shows the impact of increasing bentonite dosage on PAN for the removal of BG. With the increase in adsorbent dosage from 1 to 7 wt%, the maximum adsorption ranged from 10.76 to 35.2 mg/g at tested operating conditions. The increment in pollutant removal is caused by an increase in the availability of active sites of composite nanofibers for BG dye removal. From here, the optimal dosage of bentonite was determined to be at 7 wt% to obtain a high pollutant removal (-97%). This operating parameter was then used for the determining adsorption parameter which includes the kinetics and isotherms.

The increase in initial adsorbate concentration had a clear impact on the BG dye adsorption capacity as it increases from 50 to 250 ppm. It had an increase in adsorption capacity from 50 to 100 ppm, stating an increase in adsorption capacity of 33.75 to 64.84 mg/g and it plateaued up to 200 ppm before spiked down to 27.92 mg/g. This was the result of a decrease in pollutant removal from 97% down to 17% at the highest adsorbate concentration. This phenomenon occurred because a high initial concentration provides an important driving force in overcoming mass transfer resistance between the aqueous and the solid phases, which increases the rate at which the dye molecules pass from the bulk solution to the particle surface [29].

Although the adsorption mechanism is more efficient as the initial dye concentration increases, the percentage of the removal is higher at lower concentrations because a certain amount of bentonite can adsorb a limited amount of dye. It is of note that the removal of 100 mg/g of BG dye using PAN/Ben (64.8 mg/g) outperformed the removal performance of malachite green of 17 mg/g that was reported by [30] and the removal performance of methylene blue (20.68 mg/g) by [31]. Table 3 summarizes the results of the kinetic adsorption models used to fit with BG dye adsorption data. As a whole, the calculated equilibrium adsorption capacities and determination coefficients (R2) of the pseudo-second-order (R2 ≈ 0.96 – 0.99) fit better than the pseudo-first-order (R2 ≈ 0.64 – 0.79). The trends are confirmed by the ARE values, which were 0.26 – 0.64 and 0.01 – 0.09 for

the pseudo-first-order and pseudo-second-order respectively. This suggests that the main mechanism of BG dye adsorption is chemisorption.

The impact of pH on the adsorption of BG with PAN/Ben nanofiber are shown in Figure 6. This study shows that the pH affects the overall adsorption ability of the PAN/Ben nanofiber where it performed the best at high pH. Over the pH range of 2.3 – 10.3, the adsorption of BG onto PAN/Ben increased from 14.76 mg/g to 17.54 mg/g. The adsorption of BG onto PAN/Ben nanofiber can be attributed to the electrostatic interaction between BG and the bentonite-laden nanofiber32. At acidic pH > 2.3 to 4.1, the presence of excess H+ ions compete with the cations in the solution for the available active adsorption sites. It showed improvement as the pH becomes more basic due to the attraction of the BG ions to the adsorption site of the PAN/Ben nanofiber [32].

The adsorption isotherm at different temperatures (i.e., from 303 to 373 K) was done and the result was reported in Table 4 and Figure 8. Overall, the adsorption capacity of BG dye increased from 28.65 to 62.10 mg/g when the temperature increased from 303 to 373 K. Results from the isotherm data fitting with Langmuir and Freundlich are reported in Table 4. Langmuir model showed a better fit ($R2 \approx 0.78 – 0.99$) than the Freundlich model ($R2 \approx 0.04 – 0.97$). Furthermore, fitting the Langmuir model assumes that the adsorption that occurred was monolayer adsorption at its binding sites, homogeneous distribution of active sites on the adsorbent surface, and no adsorbate molecules interactions [32].

V. CONCLUSION

PAN/Ben nanofiber was prepared via electrospinning and used as an adsorbent for the removal of cationic brilliant green dye from water. Bentonite was found to improve the adsorption performance of PAN polymer and the best dosage for bentonite to treat 50 ppm BG dye was 7 wt% with an adsorption capacity of 33.75 mg/g. The highest adsorption capacity achieved by PAN/Ben for cationic dye removal was 64.8 mg/g. The contributing force for adsorption was found to be electrostatic interaction. The Langmuir and pseudo-second-order were the best models to correlate the BG dye adsorption data. pH and temperature were found to affect the BG dye adsorption capacity where the increase of operating variable increased the adsorption capacity.

ACKNOWLEDGMENT

The authors would like to acknowledge the Ministry of Higher Education Malaysia for Fundamental Research Grant Scheme with project code FRGS/1/2018/TK02/USM/02/6 for funding this research project. The authors also acknowledge Universiti Sains Malaysia for the support throughout this research work.

REFERENCES

[1] K. Farhana, A. S. F. Mahamude, and M. T. Mica, “The Scenario of Textile Industry in Malaysia: A Review for Potentiality,” Materials Circular Economy, vol. 4, no. 1, Dec. 2022

[2] “Emvironmental Quality Report 2020,” Ministy of Environment and Water, Malaysia.

[3] S. H. Teo et al., “Sustainable toxic dyes removal with advanced materials for clean water production: A comprehensive review,” J Clean Prod, vol. 332, no. December 2021, 2022

[4] D. Pratiwi, A. W. Indrianingsih, C. Darsih, and Hernawan, “Decolorization and Degradation of Batik Dye Effluent using Ganoderma lucidum,” IOP Conf Ser Earth Environ Sci, vol. 101, no. 1, pp. 0–7, 2017.

[5] L. Dai et al., “Calcium-rich biochar from crab shell: An unexpected super adsorbent for dye removal,” Bioresour Technol, vol. 267, no. July, pp. 510–516, 2018

[6] C. Lv et al., “Positively-charged polyethersulfone nanofibrous membranes for bacteria and anionic dyes removal,” J Colloid Interface Sci, vol. 556, pp. 492–502, 2019

[7] N. M. Mahmoodi, M. Oveisi, A. Taghizadeh, and M. Taghizadeh, “Synthesis of pearl necklace-like ZIF-8@chitosan/PVA nanofiber with synergistic effect for recycling aqueous dye removal,” Carbohydr Polym, vol. 227, no. June 2019, p. 115364, 2020

[8] M. R. S. Norsita, A. W. Zularisam, M. Nasrullah, A. R. A. Syukor, and N. W. A. Z. Najib, *“Reclamation of dye coloured of tenun textile wastewater using application of membrane technology,”* APCBEE Procedia, vol. 00, no. March 2015, pp. 000–000, 2014

[9] M. Wawrzkiewicz, M. Wiśniewska, A. Wołowicz, V. M. Gun’ko, and V. I. Zarko, “Mixed silica-alumina oxide as sorbent for dyes and metal ions removal from aqueous solutions and wastewaters,” Microporous and Mesoporous Materials, vol. 250, pp. 128–147, 2017

[10] J. Jin et al., “Cu and Co nanoparticles co-doped MIL-101 as a novel adsorbent for efficient removal of tetracycline from aqueous solutions,” Science of the Total Environment, vol. 650, pp. 408–418, 2019

[11] W. Jang, J. Yun, Y. Seo, H. Byun, J. Hou, and J. H. Kim, “Mixed dye removal efficiency of electrospun polyacrylonitrile–graphene oxide composite

membranes," Polymers (Basel), vol. 12, no. 9, pp. 1–13, 2020
[12] A. M. Khalil and A. I. Schäfer, "Cross-linked β-cyclodextrin nanofiber composite membrane for steroid hormone micropollutant removal from water," J Memb Sci, vol. 618, no. May 2020, 2021
[13] T. C. Mokhena, M. J. Mochane, A. Mtibe, M. J. John, E. R. Sadiku, and J. S. Sefadi, "Electrospun alginate nanofibers toward various applications: A review," Materials, vol. 13, no. 4, pp. 1–24, 2020
[14] N. El Messaoudi et al., "Experimental study and theoretical statistical modeling of acid blue 25 remediation using activated carbon from Citrus sinensis leaf," Fluid Phase Equilib, vol. 563, no. May, 2022
[15] H. Xue et al., "Efficient adsorption of anionic azo dyes on porous heterostructured MXene/biomass activated carbon composites: Experiments, characterization, and theoretical analysis via advanced statistical physics models," Chemical Engineering Journal, vol. 451, no. P3, p. 138735, 2023
[16] S. F. Azha et al., "Iron-modified composite adsorbent coating for azo dye removal and its regeneration by photo-Fenton process: Synthesis, characterization and adsorption mechanism interpretation," Chemical Engineering Journal, vol. 361, no. October 2018, pp. 31–40, 2019
[17] H. Çiftçi, "Removal of methylene blue from water by ultrasound-assisted adsorption using low-cost bentonites," Chem Phys Lett, vol. 802, no. May, p. 139758, 2022
[18] S. F. A. Shattar and K. Y. Foo, "Sodium salt-assisted low temperature activation of bentonite for the adsorptive removal of methylene blue," Sci Rep, vol. 12, no. 1, pp. 1–12, 2022
[19] E. G. Sogut, D. Emre, A. Bilici, N. Caliskan Kilic, and S. Yilmaz, "Porous graphitic carbon nitride nanosheets coated with polyfluorene for removal of Malachite green and Methylene blue dyes and Cu (II) ions," Mater Chem Phys, vol. 290, no. May, p. 126523, 2022
[20] L. Tian et al., "Sulfonate-modified calixarene-based porous organic polymers for electrostatic enhancement and efficient rapid removal of cationic dyes in water," J Hazard Mater, vol. 441, no. August 2022, p. 129873, 2022
[21] Q. Liu, N. Xu, L. Fan, A. Ding, and Q. Dong, "Polyacrylonitrile (PAN)/TiO2 mixed matrix membrane synthesis by thermally induced self-crosslinking for thermal and organic-solvent resistant filtration," Chem Eng Sci, vol. 228, p. 115993, 2020
[22] Z. Zhang, N. Chu, Y. Shen, C. Li, and R. Liu, "Enhancing U(VI) adsorptive removal via amidoximed polyacrylonitrile nanofibers with hierarchical porous structure," Colloid Polym Sci, vol. 299, no. 1, pp. 25–35, 2021
[23] J. Ma, J. Qi, C. Yao, B. Cui, T. Zhang, and D. Li, "A novel bentonite-based adsorbent for anionic pollutant removal from water," Chemical Engineering Journal, vol. 200–202, pp. 97–103, 2012
[24] [24] Z. Yuan, X. Cheng, L. Zhong, R. Wu, and Y. Zheng, "Preparation, characterization and performance of an electrospun carbon nanofiber mat applied in hexavalent chromium removal from aqueous solution," J Environ Sci (China), vol. 77, pp. 75–84, 2019
[25] S. A. Obaid, "Langmuir, Freundlich and Tamkin Adsorption Isotherms and Kinetics for the Removal Aartichoke Tournefortii Straw from Agricultural Waste," J Phys Conf Ser, vol. 1664, no. 1, 2020
[26] J. P. Simonin, "On the comparison of pseudo-first order and pseudo-second order rate laws in the modeling of adsorption kinetics," Chemical Engineering Journal, vol. 300, no. August, pp. 254–263, 2016
[27] R. Reddy T, K. S, E. T, and L. Reddy S, "Spectroscopic Characterization of Bentonite," J Lasers Opt Photonics, vol. 04, no. 03, 2017
[28] N. Banik et al., "Synthesis and characterization of organoclay modified with cetylpyridinium chloride," Bangladesh Journal of Scientific and Industrial Research, vol. 50, no. 1, pp. 65–70, 2015
[29] C. Leodopoulos, D. Doulia, and K. Gimouhopoulos, "Adsorption of cationic dyes onto bentonite," Separation and Purification Reviews, vol. 44, no. 1. Taylor and Francis Inc., pp. 74–107, 2014.
[30] A. A. Adeyi, S. N. A. M. Jamil, L. C. Abdullah, and T. S. Y. Choong, "Adsorption of malachite green dye from liquid phase using hydrophilic thiourea-modified poly(acrylonitrile- co -acrylic acid): Kinetic and isotherm studies," J Chem, vol. 2019, 2019
[31] T. Li, L. Liu, Z. Zhang, and Z. Han, "Preparation of nanofibrous metal-organic framework filter for rapid adsorption and selective separation of cationic dye from aqueous solution," Sep Purif Technol, vol. 237, Apr. 2020
[32] M. L. F. A. de Castro, M. L. B. Abad, D. A. G. Sumalinog, R. R. M. Abarca, P. Paoprasert, and M. D. G. de Luna, "Adsorption of Methylene Blue dye and Cu(II) ions on EDTA-modified bentonite: Isotherm, kinetic and thermodynamic studies," Sustainable Environment Research, vol. 28, no. 5, pp. 197–205, Sep. 2018